



Paper Type: Original Article

## Homotopy Analysis Method (HAM) of Nanofluid Natural Convection over a Cone in Porous Media for Nuclear Waste

Hashem Saberi Najafi<sup>\*</sup>, Jafar Biazar<sup>1</sup>

<sup>1</sup> Department of Applied Mathematics and Computer Science, Faculty of Mathematical Sciences, University of Guilan, Rasht, Gilan, Iran; hnajafi@guilan.ac.ir; biazar@guilan.ac.ir.

Citation:

Received: 25 January 2024

Revised: 26 April 2024

Accepted: 17 June 2024

Saberi Najafi, H., & Biazar, J. (2024). Homotopy analysis method (HAM) of nanofluid natural convection over a cone in porous media for nuclear waste. *Mechanical Technology and Engineering Insights*, 1(4), 215-230.


### Abstract


In this paper, we tried to find a solution for the quick transfer of atomic dump (nuclear wastes) from pools of cool water to dry stores in order to reduce the environmental and financial expenses of burying atomic waste considerably. So the velocity of heat transfer should be increased from the atomic waste materials to the area outside the container. Therefore, in Bottom of the pool, we can embed space with conical fins (vertically) applied within it, and inside the space, such fins are in a porous medium, and natural convection flow of Newtonian nanofluid passes upon it. In this research, we study the velocity of heat transfer by using such a special space. In this research, free convection boundary layer flow on a vertical cone in a porous medium for Newtonian nanofluid with Analytical solutions has been studied. Similarity solution for a cone subjected to Consideration boundary conditions is a nonlinear ordinary differential equation, which has been solved through the Homotopy Analysis Method (HAM). The obtained analytical solution, in comparison with the numerical ones, represents remarkable accuracy. The results also indicate that HAM can provide us with a convenient way to control and adjust the convergence region. By the way, we also calculate the Nusselt number, which is an important parameter in heat transfer, by obtaining an analytical solution using HAM.

**Keywords:** Nuclear wastes, Homotopy analysis method, Porous media, Newtonian nanofluid, Similarity solution, Ordinary differential equations.

## 1 | Introduction

The natural convection flow over a surface embedded in saturated porous media is encountered in many engineering problems such as the design of pebble-bed nuclear reactors, ceramic processing, crude oil drilling, geothermal energy conversion, use of fibrous material in the thermal insulation of buildings, catalytic reactors

 Corresponding Author: hnajafi@guilan.ac.ir

 <https://doi.org/10.48313/mtei.v1i4.69>



Licensee System Analytics. This article is an open access article distributed under the terms and conditions of the Creative Commons Attribution (CC BY) license (<http://creativecommons.org/licenses/by/4.0>).

and compact heat exchangers, heat transfer from storage of agricultural products which generate heat as a result of metabolism, petroleum reservoirs, storage of nuclear wastes, etc. Consumed atomic fuels (nuclear wastes) are kept protectively in special small pools. The water within each small pool, in addition to cooling the Uranium, prevents the exit of radioactive radiation. After passing several decades, the fuels, whose temperature and radiation features have now reduced noticeably, exit from the small pools and are transferred to dry stores. In these stores, fuels are kept in metallic or concrete containers; also, in this phase, radiation made by fuels is still dangerous. In this phase, the duration of protecting fuels in relation to the kind of fuel can be variable from several years to decades, but anyway, fuels should stay in this phase long enough until their temperature and radiation levels reach a standard level.

According to Olander [1], one of the researchers at MIT University of America, in this project, the consumed fuel, instead of being transferred to a dump, would be transferred to a big source of energy comparable to large strategic stores of oil. Storage of consumed fuel in dry reservoirs for several decades causes them to cool to a safe temperature, and after that, they can be buried in a permanent organization for burying dumps, which is cheaper and smaller than a recent organization, or the consumed fuel can be retrieved and reused.

In this research, we tried to find a solution for the quick transfer of atomic dump from pools of cool water to dry stores in order to reduce the environmental and financial expenses of burying atomic waste considerably. For this reason, if the duration of protecting atomic waste materials in pools is reduced, the velocity of heat transfer should be increased from the atomic waste materials to the area outside the container. Therefore, at the Bottom of the pool, *Fig. 1*, we can embed a space in which conical fins (vertically) are applied, and inside of the space, such fins are in a porous medium, and natural convection flow of Newtonian nanofluid passes upon it. In this research, we study the velocity of heat transfer by using such a special space.

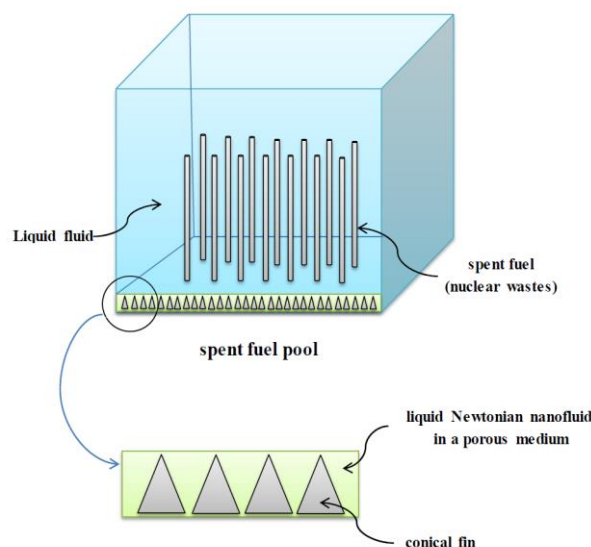


**Fig. 1. Bottom of the spent fuel pool.**

The derivation of the empirical equations that govern the flow and heat transfer in a porous medium has been discussed in [2]. The natural convection on vertical surfaces in porous media has been studied using Darcy's law by a number of authors [3–5]. Boundary layer analysis of natural convection over a cone has been investigated by Yih [6].

Murthy and Singh [7] obtained the similarity solution for non-Darcy mixed convection about an isothermal vertical cone with fixed apex half angle, pointing downwards in a fluid-saturated porous medium with uniform free stream velocity. However, a semi-similar solution of an unsteady mixed convection flow over a rotating cone in a rotating viscous fluid has been obtained by Roy and Anilkumar [8]. The laminar steady nonsimilar natural convection flow of gases over an isothermal vertical cone has been investigated by Takhar et al. [9].

The development of unsteady mixed convection flow of an incompressible laminar viscous fluid over a vertical cone has been investigated by Singh and Roy [10] when the fluid in the external stream is set into motion impulsively, and at the same time, the surface temperature is suddenly changed from its ambient temperature. An analysis has been carried out by Kumari and Nath [11] to study the non-Darcy natural convection flow of non-Newtonian fluids on a vertical cone embedded in a saturated porous medium with power-law variation of the wall temperature/concentration or heat/mass flux and suction/injection. Cheng [12] focused on the problem of natural convection from a vertical cone in a porous medium with mixed thermal boundary conditions, Soret and Dufour effects, and with variable viscosity.

The conventional heat transfer fluids, including oil, water, and ethylene glycol, etc., are poor heat transfer fluids, since the thermal conductivity of these fluids plays an important role in the heat transfer coefficient between the heat transfer medium and the heat transfer surface. An innovative technique for improving heat transfer by using ultrafine solid particles in the fluids has been used extensively during the last several years. Choi and Eastman [13] introduced the term "nanofluid" to refer to these kinds of fluids by suspending nanoparticles in the base fluid.

Khanafer et al. [14] investigated the heat transfer enhancement in a two-dimensional enclosure utilizing nanofluids. The convective boundary-layer flow over vertical plates, stretching sheets, and moving surfaces has been studied by numerous researchers and in the review papers Buongiorno [15], Daungthongsuk and Wongwises [16], Oztop and Abu-Nada [17], Nield and Kuznetsov [18], [19] Ahmad and Pop [20], Khan and Pop [21], Kuznetsov and Nield [22], and Bachok et al. [23].

In recent years, significant research efforts have been devoted to the study of nanofluid flow and heat transfer over vertical cones embedded in porous media. Alqurashi and Hassan [24] employed artificial intelligence neural network modeling to investigate radiative nanofluid flow via a vertical cone in a porous medium with activation energy effects. Gomathi and De [25] analyzed entropy optimization on EMHD Casson Williamson penta-hybrid nanofluid over a porous exponentially vertical cone.

Kodi et al. [26] examined the influence of MHD mixed convection flow for Maxwell nanofluid through a vertical cone with porous material in the presence of variable heat conductivity and diffusion. Ragulkumar et al. [27] studied natural convective dissipative different nanofluid flow past a vertical cone with heat and mass transfer. Yashodha et al. [28] analyzed the convective flow of water-ethylene glycol (50:50) based nanofluid over a spinning down-pointing vertical cone in a Darcy porous medium.

Rana et al. [29] revisited the Cheng–Minkowycz problem for quadratic convective and radiative heat transfer in a nanofluid saturated porous medium. Hashim [30] investigated natural convection inside nanofluid superposed wavy porous layers using the local thermal non-equilibrium model. Furthermore, recent studies have explored chemically reactive magnetized flow of viscoplastic nanofluid through a vertical cone considering non-Darcy porous media [31], and mathematical modeling of SWCNT-and MWCNT-based nanofluid flow with thermal and chemically reactive effects inside a porous vertical cone [32]. Comprehensive reviews on nanofluid heat transfer in porous media have also been published [33].

From the literature survey, the primary aim of this work is to study the free convection boundary-layer flow past a vertical cone embedded in a porous medium filled with a nanofluid, the basic fluid being a Newtonian fluid, by using similarity transformations. The Ordinary differential equations (ODE) are solved by the Homotopy Analysis Method (HAM). The effects of the parameters governing the problem are studied and discussed.

## 2 | Mathematical Formulation of the Problem

Consider the problem of natural convection about a downward -pointing vertical cone of half angle  $\varphi$  embedded in a porous medium saturated with a Newtonian power-law nanofluid. The origin of the coordinate system is placed at the vertex of the full cone, with  $x$  being the coordinate along the surface of the cone, measured from the origin, and  $y$  being the coordinate perpendicular to the conical surface *Fig. 2*. The

temperature of the porous medium on the surface of the cone is kept at constant temperature  $T_w$ . The ambient porous medium temperature is held at constant temperature  $T_\infty$ . The nanofluid properties are assumed to be constant except for density variations in the buoyancy force term. The thermo-physical properties of the Newtonian nanofluid are given in *Table 1* (see Oztop and Abu-Nada [17]).

Assuming that the thermal boundary layer is sufficiently thin compared with the local radius, the equations governing the problem of Darcy flow through a homogeneous porous medium saturated with power-law Newtonian nanofluid near the vertical cone can be written in two-dimensional Cartesian coordinates  $(x,y)$  as:

$$\frac{\partial(r^a u)}{\partial x} + \frac{\partial(r^a v)}{\partial y} = 0. \quad (1)$$

$$u = \frac{(\rho\beta)_{nf}}{\mu_{nf}} K_d g (T - T_\infty) \cos \varphi. \quad (2)$$

$$u \frac{\partial T}{\partial x} + v \frac{\partial T}{\partial y} = \left( \frac{k}{\rho c_p} \right)_{nf} \frac{\partial^2 T}{\partial y^2}, \quad (3)$$

where  $u$  and  $v$  are the volume-averaged velocity components in the  $x$  and  $y$  directions, respectively,  $T$  is the volume-averaged temperature, and  $g$  is the gravitational acceleration.  $a=\varphi=0$  corresponds to flow over a vertical flat plate.  $A = \varphi = 1$  corresponds to flow over a vertical cone. Property  $\rho_{nf}$  and  $\mu_{nf}$  are the density and effective viscosity of the nanofluid.  $K_d$  is the modified permeability of the porous medium. Furthermore,  $\alpha_{nf}$  and  $\beta_{nf}$  are the equivalent thermal diffusivity and the thermal expansion coefficient of the saturated porous medium, which are defined as (see Khanafer et al. [14]):

$$\begin{aligned} \rho_{nf} &= (1-\phi)\rho_f + \phi\rho_s, \\ \mu_{nf} &= \frac{\mu_f}{(1-\phi)^{2.5}}, \\ \alpha_{nf} &= \frac{k_{nf}}{(\rho c_p)_{nf}}, \\ (\rho c_p)_{nf} &= (1-\phi)(\rho c_p)_f + \phi(\rho c_p)_s, \end{aligned} \quad (4)$$

$$\frac{k_{nf}}{k_f} = \frac{(k_s + 2k_f) - 2\phi(k_f - k_s)}{(k_s + 2k_f) + 2\phi(k_f - k_s)}.$$

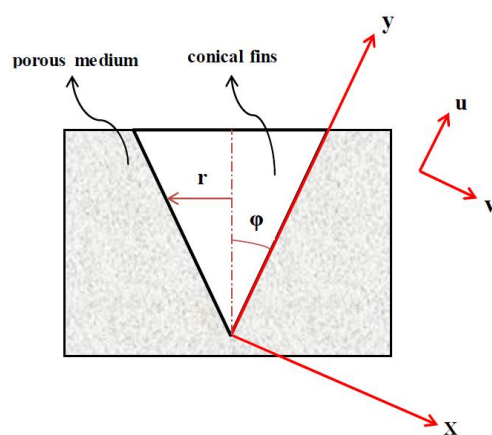


Fig. 1. A schematic diagram of the physical model.

Table 1. Thermo-physical properties of water and nanoparticles [17].

Number	Material	Physical Properties			
		$\rho$ (kg/m <sup>3</sup> )	$C_p$ (J/KgK)	$k$ (W/mK)	$\beta \times 10^5$ (K <sup>-1</sup> )
1	Pure water	997.1	4179	0.613	21
2	Copper (Cu)	8933	385	401	1.67
3	Silver (Ag)	10500	235	429	1.89
4	Alumina (Al <sub>2</sub> O <sub>3</sub> )	3970	765	40	0.85
5	Titanium (TiO <sub>2</sub> )	4250	686.2	8.9538	0.9

Here  $\phi$  is the solid volume fraction. The associated boundary conditions of Eqs. (1)-(3) can be written as:

$$\begin{aligned} u &= 0, \quad T \rightarrow T_\infty \quad \text{as } y \rightarrow \infty, \\ v &= 0, \quad T = T_w \quad \text{at } y = 0, \end{aligned} \quad (5)$$

where  $\mu_f$  is the viscosity of the basic fluid,  $\rho_f$  and  $\rho_s$  are the densities of the pure fluid and nanoparticle, respectively,  $(\rho C_p)_f$  and  $(\rho C_p)_s$  are the specific heat parameters of the base fluid and nanoparticle, respectively,  $k_f$  and  $k_s$  are the thermal conductivities of the base fluid and nanoparticle, respectively. The local radius to a point in the boundary layer  $r$  can be represented by the local radius of the vertical cone  $r = x \sin \varphi$ . By introducing the following non-dimensional variables:

$$\eta = \frac{y}{x} \text{Ra}_x^{0.5}. \quad (6)$$

$$f(\eta) = \frac{\psi(x, y)}{\alpha_f r^a \text{Ra}_x^{0.5}}. \quad (7)$$

$$\theta(\eta) = \frac{T - T_\infty}{T_w - T_\infty}.$$

The continuity equation is automatically satisfied by defining a stream function  $\Psi(x, y)$  such that:

$$r^a u = \frac{\partial(\Psi)}{\partial y}, \quad r^a v = -\frac{\partial(\Psi)}{\partial x}, \quad (8)$$

where;

$$\text{Ra}_x = \left( \frac{x}{\alpha_f} \right) \left[ \frac{(\beta \rho)_f g K_d \cos \varphi \Delta T}{\mu_f} \right]. \quad (9)$$

Integration of the Momentum (2) we have:

$$\frac{\mu_{nf}}{\mu_f} u = \frac{(\rho \beta)_{nf} K_d g \cos \varphi}{\mu_f} (T - T_\infty). \quad (10)$$

Substituting Variables (6) into Eqs. (1)-(5) with Eq. (10), we obtain the following system of ODE:

$$\frac{1}{(1-\phi)^{2.5} \left[ (1-\phi) + \phi \frac{(\rho \beta)_s}{(\rho \beta)_f} \right]} f'(\eta) = \theta(\eta). \quad (11)$$

$$\frac{\left( \frac{(k_s + 2k_f) - 2\phi(k_f - k_s)}{(k_s + 2k_f) + 2\phi(k_f - k_s)} \right)}{\left( (1-\phi) + \phi \frac{(\rho c_p)_s}{(\rho c_p)_f} \right)} \theta''(\eta) + \left( \frac{1}{2} + a \right) f(\eta) \theta'(\eta) = 0. \quad (12)$$

Along with the boundary conditions:

$$\begin{aligned} f(0) &= 0, & \theta(0) &= 1, \\ f'(\infty) &= 0, & \theta'(\infty) &= 0. \end{aligned} \quad (13)$$

Finally from Eqs. (10)-(12) we have:

$$\begin{aligned} \text{ODE:} \quad & \left(\frac{1}{2} + a\right) \left[ (1 - \phi) + \phi \frac{(\rho c_p)_s}{(\rho c_p)_f} \right] f(\eta) f''(\eta) + \\ & \left[ \frac{(k_s + 2k_f) - 2\phi(k_f - k_s)}{(k_s + 2k_f) + 2\phi(k_f - k_s)} \right] f'''(\eta) = 0. \end{aligned} \quad (14)$$

$$\text{B.C: } f(0) = 0, f'(0) = 1, f'(\infty) = 0.$$

It is of interest to obtain the value of the local Nusselt number, which is defined as:

$$\text{Nu}_x = \frac{q_w x}{k(T_w - T_\infty)}, \quad (15)$$

where  $q_w$  for the case of prescribed wall temperature can be computed from:

$$q_w = -k \left. \frac{\partial T}{\partial y} \right|_{y=0} \quad (16)$$

From Eq. (15), Eq. (16), Eq. (6), and Eq. (8) it follows that the local Nusselt number is given by:

$$\text{Nu}_x = \text{Ra}_x^{0.5} [-\theta'(0)]. \quad (17)$$

### 3 | Applications

Consider the governing equation of Newtonian nanofluid flow and heat transfer of a cone embedded in a porous medium, which is expressed by Eq. (13), considering the boundary conditions. Consider the equation that prescribes the wall temperature case, which is expressed by Eq. (13). We define a nonlinear operator as follows:

$$\begin{aligned} \mathcal{N}[f(\eta; q)] &= \left(\frac{1}{2} + a\right) \left[ (1 - \phi) + \phi \frac{(\rho c_p)_s}{(\rho c_p)_f} \right] f(\eta; q) \frac{\partial^2 f(\eta; q)}{\partial \eta^2} \\ &+ \left[ \frac{(k_s + 2k_f) - 2\phi(k_f - k_s)}{(k_s + 2k_f) + 2\phi(k_f - k_s)} \right] \frac{\partial^3 f(\eta; q)}{\partial \eta^3}, \end{aligned} \quad (18)$$

where  $q \in [0, 1]$  is the embedding parameter,  $h \neq 0$  is a nonzero auxiliary parameter. As the embedding parameter increases from 0 to 1,  $U(\eta, q)$  varies from the initial guess  $U_0(\eta)$  to the exact solution  $U(\eta)$ ;

$$f(\eta; 0) = U_0(\eta), f(\eta; 1) = U(\eta). \quad (19)$$

Expanding  $f(\eta, q)$  in a Taylor series with respect to  $q$ , we have:

$$f(\eta; q) = U_0(\eta) + \sum_{m=1}^{+\infty} U_m(\eta) q^m, \quad (20)$$

where

$$U_m(\eta) = \frac{1}{m!} \left. \frac{\partial^m f(\eta; q)}{\partial q^m} \right|_{q=0} \quad (21)$$

HAM can be expressed by many different base functions [24], according to the governing equation; it is straightforward to use a set of base functions:

$$\{\eta^p e^{-m\eta} | p, m = 0, 1, 2, 3, \dots\}. \quad (22)$$

In the form

$$U(\eta) = \sum_{m=1}^{\infty} \sum_{p=1}^{\infty} b_p \eta^p e^{-m\eta}. \quad (23)$$

That  $b_n$  is a coefficient to be determined. Besides determining a set of base functions, the auxiliary function  $H(\eta)$ , initial approximation  $U_0(\eta)$ , and the auxiliary linear operator  $L$  must be chosen in such a way that all solutions of the corresponding high-order deformation equations exist and can be expressed by this set of base functions, and the other expressions, such as  $\eta^n \sin(m\eta)$ , must be avoided. This provides us with the so-called rule of solution expression [34]. It should be noticed that terms like  $\eta^p e^{-m\eta} | p, m > 0$  do not belong to the so-called secular terms such as  $(\eta^p \sin(m\eta), \eta^p \cos(m\eta))$  because the term  $\eta^p e^{-m\eta} | p, m > 0$  tends to zero as  $\eta \rightarrow \infty$  [34]. We choose a linear operator, as below:

$$L[f(\eta; q)] = \frac{\partial^3 f(\eta; q)}{\partial \eta^3}. \quad (24)$$

With the property

$$L[c_1 + c_2 \eta + c_3 e^{-\eta}] = 0, \quad (25)$$

where  $c_1, c_2$  and  $c_3$  are integral constants. We must choose an initial guess of  $U(\eta)$  so that it prevents divergence of answers. According to the discussed limitation and under the rule of solution expression and initial conditions, we choose an initial guess in the form:

$$U_0(\eta) = c_1 + c_2 \eta + c_3 e^{-\eta}. \quad (26)$$

$$U_0(\eta) = 1 - \exp(-\eta). \quad (27)$$

The zero-order deformation equation is:

$$(1 - q)L[f(\eta; q) - U_0(s)] = qhH(s)N[f(\eta; q)]. \quad (28)$$

$$f(0; q) = 0, \frac{\partial f(\infty; q)}{\partial \eta} = 0, \frac{\partial^2 f(\infty; q)}{\partial \eta^2} = 0. \quad (29)$$

According to the rule of solution expression denoted by Eq. (24) and from Eq. (28), the auxiliary function  $H(\eta)$  can be chosen as follows:

$$H(\eta) = \eta^p e^{m\eta}. \quad (30)$$

Differentiating (28),  $m$  times with respect to the embedding parameter  $q$  and then setting  $q = 0$ , and finally dividing them by  $m!$ , and from Eq. (19), and Eq. (26), we have the so-called  $m$ th-order deformation equation for  $m \geq 1$ :

$$U_m(\eta) = \chi_m U_{m-1}(\eta) + \hbar \int_0^{\eta} \int_0^{\mu} \int_0^{\tau} H(\eta) e^{\eta} R_m(\bar{U}_{m-1}) d\eta d\tau d\mu + c_1 + c_2 \eta + c_3 e^{-\eta}. \quad (31)$$

$$U_m(0) = 0, (U_m)'(\infty) = 0, (U_m)''(\infty) = 0,$$

where

$$R_m(\vec{U}_{m-1}) = \left( \frac{(k_s + 2k_f) - 2\phi(k_f - k_s)}{(k_s + 2k_f) + 2\phi(k_f - k_s)} \right) \frac{\partial^3 \vec{U}_{m-1}(\eta)}{\partial \eta^3} + \left( \frac{1}{2} + a \right) \left( (1 - \phi) + \phi \frac{(\rho c_p)_s}{(\rho c_p)_f} \right) \left( \sum_{z=0}^{m-1} \vec{U}_z(\eta) \left( \frac{\partial^2 \vec{U}_{m-1-z}(\eta)}{\partial \eta^2} \right) \right). \quad (32)$$

and

$$X_m = \begin{cases} 0, & m \leq 1, \\ 1 & m > 1. \end{cases} \quad (33)$$

It is time to choose  $H(\eta)$  uniquely under the rule of solution expression and the rule of coefficient ergodicity [24]. So we have to choose  $\{p=0, m=-1\}$ . Consequently, the corresponding auxiliary function was determined uniquely,  $H(\eta)=e^{-\eta}$ . We now successively obtain:

$$U_0(\eta) = 1 - e^{-\eta}.$$

$$U_1(\eta) =$$

$$\begin{aligned} & (-0.05711939723 + 0.06126805522e^{-1.x} + 0.007293506583e^{-3.x} \\ & - 0.008242682212e^{-4.x} - 0.01193332704e^{-5.x} \\ & - 0.001904150650e^{-6.x} + 0.01071045486e^{-2.x} \\ & - 0.00007245953384e^{-7.x}) h^3 + (-0.2740431288 \\ & - 0.004137625704e^{-5.x} - 0.05846724927e^{-4.x} \\ & + 0.05802396765e^{-2.x} + 0.3486814590e^{-1.x} \\ & - 0.07005742290e^{-3.x}) h^2 + (-0.5422444335 \\ & + 1.001446451e^{-1.x} - 0.3761596017e^{-2.x} \\ & - 0.08304241593e^{-3.x}) h + 1. - 1. e^{-x} \end{aligned} \quad (34)$$

### 3 | Convergence of Homotopy Analysis Method Solution

We should ensure that the solution converges. Note that we still have freedom to choose the auxiliary parameter has pointed out by Liao [24], the convergence region and rate of solution series can be adjusted and controlled by means of the auxiliary parameter  $h$ .

In general, by means of the so-called  $h$ -curve, it is straightforward to choose an appropriate range for  $h$  that ensures the convergence of the solution series. To influence of  $h$  on the convergence of solution, we plot the so-called  $h$ -curves of  $f(\eta)$ , by 17th-order approximation of solution for Cu-water, Ag-water,  $Al_2O_3$ -water, and  $TiO_2$ -water in  $\phi=0.1$ , as shown in *Fig. 3-6*. It is easy to discover that the valid region of  $h$  is  $-1.5 \leq h \leq 0$ . Moreover, increasing the order of approximation increases the range of acceptable values of  $h$ .

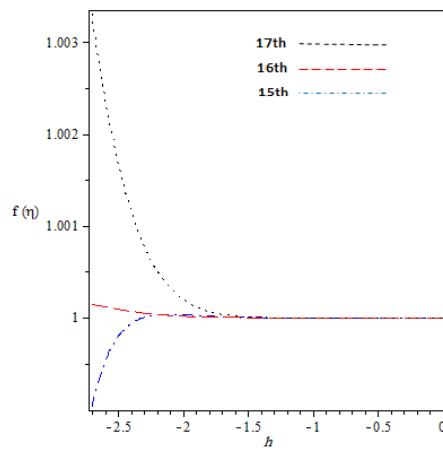


Fig. 3. The h-curve by 17th-order approximation for Cu-water.  $\Phi=0.1$ .

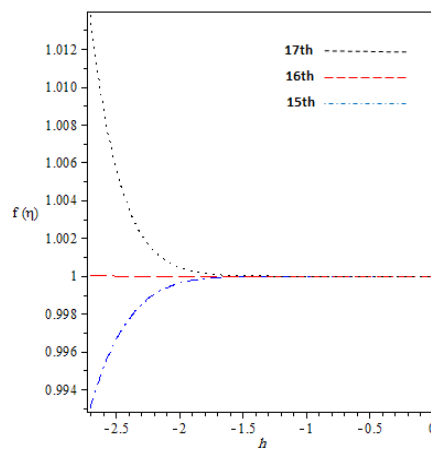


Fig. 4. The h-curve by 17th-order approximation for Ag-water.  $\Phi=0.1$ .

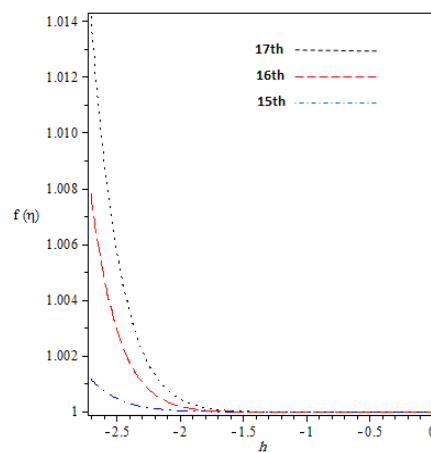


Fig. 5. The h-curve by 17th-order approximation for Al<sub>2</sub>O<sub>3</sub>-water.  $\Phi=0.1$ .

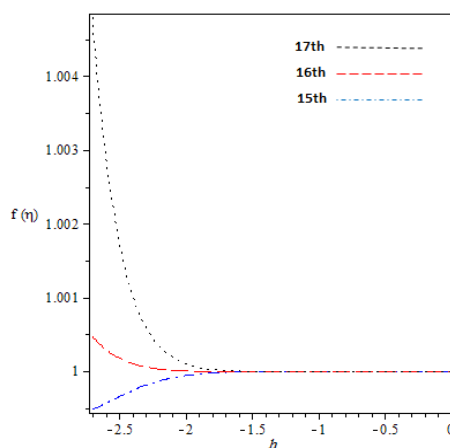


Fig. 6. The h-curve by 17th-order approximation for TiO<sub>2</sub>-water.  $\Phi=0.1$ .

### 4 | Results and Discussion

In this study, we have presented similarity reductions for the effect of a nanoparticle volume fraction on the free convection flow of nanofluids over a vertical cone via similarity transformations. The HAM solutions of the resulting similarity reductions are obtained for the original variables, which are shown in Eq. (13) along with the boundary Conditions (14), by using the HAM. The physical quantity of interest here is the Nusselt number  $Nu_x$ , and it is obtained and shown in Eq. (17). The distributions of the velocity  $f'(\eta)$ , Eq. (13) and the Nusselt number in the cases of Cu-water, Ag-water, Al<sub>2</sub>O<sub>3</sub>-water, and TiO<sub>2</sub>-water are shown in Figs. 7–14. The computations are carried out for various values of the nanoparticles' volume fraction for different types of nanoparticles, when the base fluid is water. Nanoparticles volume fraction  $\phi$  is varied from 0 to 0.2. The nanoparticles used in the study are from Copper (Cu), Silver (Ag), Alumina (Al<sub>2</sub>O<sub>3</sub>), and Titanium oxide (TiO<sub>2</sub>).

Table 2 depicts the heat transfer rate  $\theta'(0)$  for various values of nanoparticles volume fraction  $\phi$  for different types of nanoparticles when the base fluid is water. Figures show the effects of the nanoparticle volume fraction  $\phi$  on the velocity distribution in the cases of Cu-water, Ag-water, Al<sub>2</sub>O<sub>3</sub>-water, and TiO<sub>2</sub>-water when  $\phi = 0, 0.025, 0.05, 0.075, 0.1, 0.125, 0.15, 0.175, 0.2$ . It is noted that the velocity along the cone increases with the nanoparticle volume fraction in the four cases; the velocity distribution in the case of Ag-water is larger than that for Cu-water, Al<sub>2</sub>O<sub>3</sub>-water, and TiO<sub>2</sub>-water. We can show that the change of the velocity distribution when we use different types of nanoparticles from Figs. 7-10, which depicts that the Ag-nanoparticles are the highest when the base fluid is water and when  $\phi = 0.1$ . Thus, the presence of the nanoparticles' volume fraction increases the momentum boundary layer thickness.

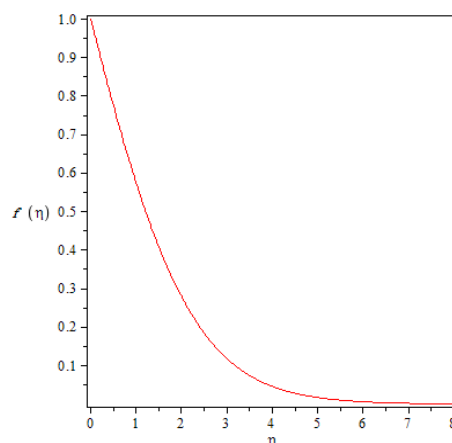


Fig. 7. Effect of  $\phi=0.1$  on velocity distribution  $f'(\eta)$  in the case of Cu-water.

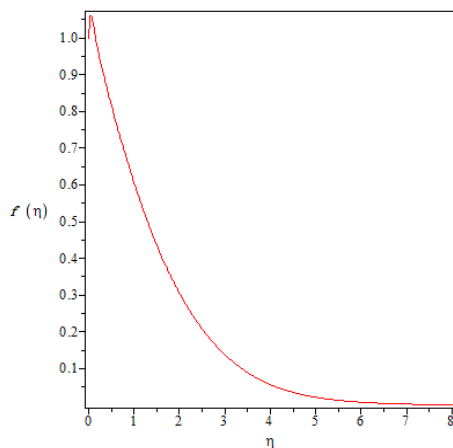


Fig. 8. Effect of  $\phi=0.1$  on velocity distribution  $f'(\eta)$  in the case of Ag-water.

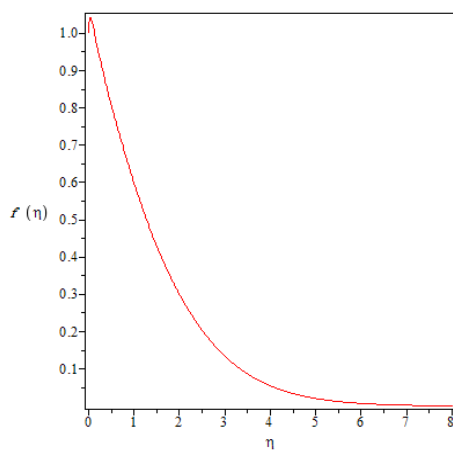


Fig. 9. Effect of  $\phi=0.1$  on velocity distribution  $f'(\eta)$  in the case of  $\text{Al}_2\text{O}_3$ -water.

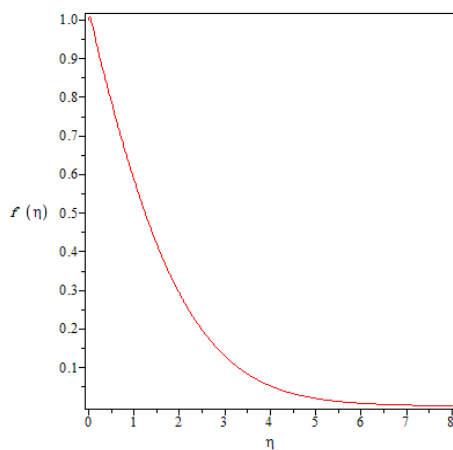
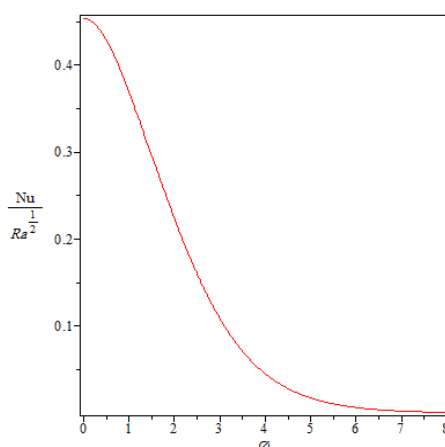


Fig. 10. Effect of  $\phi=0.1$  on velocity distribution  $f'(\eta)$  in the case of  $\text{TiO}_2$ -water.

**Table 2. Values of  $-\theta'(0)$  for various values of  $\phi$ .**

$\phi$	Material			
	Copper (Cu)	Silver (Ag)	Alumina (Al <sub>2</sub> O <sub>3</sub> )	Titanium (TiO <sub>2</sub> )
0.025	0.45575120	0.45465451	0.45573793	0.45706440
0.05	0.45498519	0.45279643	0.45494967	0.45761224
0.075	0.45421398	0.45093107	0.45415178	0.45814745
0.1	0.45345267	0.44906030	0.45335467	0.45867323
0.125	0.45268364	0.44718110	0.45254246	0.45918932
0.15	0.45190084	0.44529991	0.45173114	0.45969944
0.175	0.45113710	0.44342033	0.45092252	0.46018894
0.2	0.45036219	0.44152570	0.45011013	0.46067544

Figs. 11-14 shows the variation of the reduced Nusselt number with the nanoparticles volume fraction  $\phi$  for the selected types of nanoparticles. It is clear that the heat transfer rates decrease with the increase in the nanoparticles volume fraction  $\phi$ . The change in the reduced Nusselt number is found to be lower for higher values of the parameter  $\phi$ . It is observed that the reduced Nusselt number is higher in the case of Ag-nanoparticles and next unanoparticles, TiO<sub>2</sub>-nanoparticles, and Al<sub>2</sub>O<sub>3</sub>-nanoparticles. Also, Figs. 11-14 and Table 2 show that the values of  $\theta'(0)$  change with Newtonian nanofluid changes, namely, we can say that the shear stress and heat transfer rate change by taking different types of nanofluid. Furthermore, this depicts that the Newtonian nanofluids will be very important materials in the heating and cooling processes.



**Fig. 11. Effects of the nanoparticle volume fraction  $\phi$  on dimensionless heat transfer rates in the case of Cu-water.**

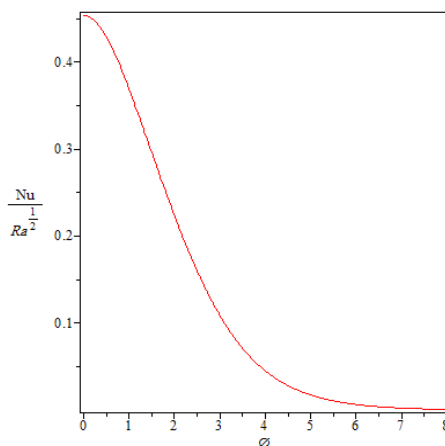


**Fig. 12. Effects of the nanoparticle volume fraction  $\phi$  on dimensionless heat transfer rates in the case of Ag-water.**

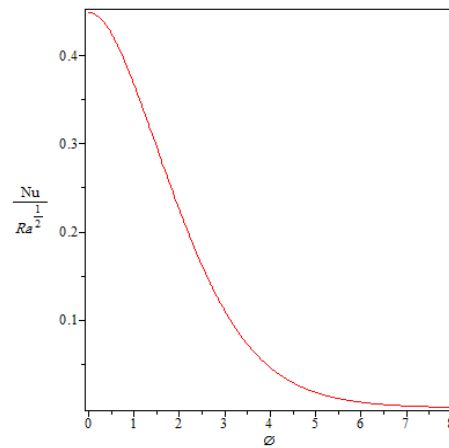


**Fig. 13.** Effects of the nanoparticle volume fraction  $\phi$  on dimensionless heat transfer rates in the case of  $\text{Al}_2\text{O}_3$ -water.

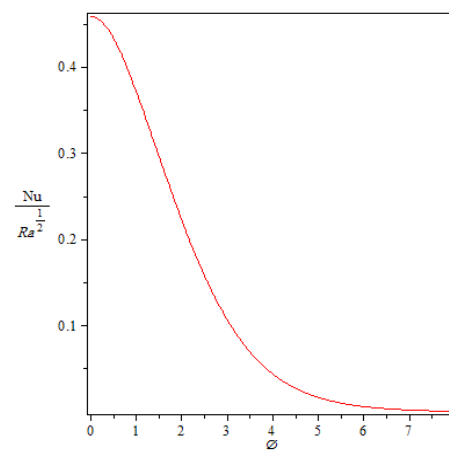


**Fig. 14.** Effects of the nanoparticle volume fraction  $\phi$  on dimensionless heat transfer rates in the case of  $\text{TiO}_2$ -water.

## 5 | Conclusion

In this work, an analytical analysis on the steady free convective flow of Newtonian nanofluids past a vertical cone placed in a porous medium was considered, with the objective of improving the heat transfer rate of the system as required for removing heat in the cooling of spent nuclear fuel pools. By employing the similarity transformation technique, the governing partial differential equations were transformed to ordinary nonlinear differential equations, which were solved successfully by means of the HAM and found to give very good results with controllable convergence using the auxiliary parameter  $h$ .

The main conclusions drawn are as follows:

- I. Increased velocity: The increase in nanoparticle volume fraction ( $\varphi$ ) leads to increased velocity for all the nanofluids considered (Cu-water, Ag-water,  $\text{Al}_2\text{O}_3$ -water, and  $\text{TiO}_2$ -water).
- II. Decreased heat transfer: The Nusselt number decreases with increasing  $\varphi$  for all nanofluids, thus implying increased thickness of the thermal boundary layer.
- III. Optimized nanofluid application: Ag-water nanofluid has maximum cooling Effect, while  $\text{Al}_2\text{O}_3$ -water nanofluid gives maximum heating effect.

IV. Practical application of this study: Passive cooling processes, such as porous media with vertical cones, can be employed for the rapid cooling of spent nuclear fuel pools at reduced costs.

## Conflict of Interest

The authors have no relevant financial or non-financial interests to disclose.

## Data Availability

The research data supporting this study are available upon reasonable request from the corresponding author.

## Funding

This research did not receive any specific grant from funding agencies in the public, commercial, or not-for-profit sectors.

## References

- [1] Olander, D. (2009). Nuclear fuels—Present and future. *Journal of nuclear materials*, 389(1), 1–22. <https://doi.org/10.1016/j.jnucmat.2009.01.297>
- [2] Ingham, D. B., & Pop, I. (2005). *Transport phenomena in porous media III* (Vol. 3). Elsevier. <https://doi.org/10.1016/B978-0-08-042843-7.X5000-4%0A%0A>
- [3] Nield, D. A., & Kuznetsov, A. V. (2008). Natural convection about a vertical plate embedded in a bidisperse porous medium. *International journal of heat and mass transfer*, 51(7), 1658–1664. <https://doi.org/10.1016/j.ijheatmasstransfer.2007.07.011>
- [4] Mahdy, A., & Hady, F. M. (2009). Effect of thermophoretic particle deposition in non-Newtonian free convection flow over a vertical plate with magnetic field effect. *Journal of non-newtonian fluid mechanics*, 161(1), 37–41. <https://doi.org/10.1016/j.jnnfm.2009.04.003>
- [5] Ibrahim, F. S., Hady, F. M., Abdel-Gaied, S. M., & Eid, M. R. (2010). Influence of chemical reaction on heat and mass transfer of non-Newtonian fluid with yield stress by free convection from vertical surface in porous medium considering Soret effect. *Applied mathematics and mechanics*, 31(6), 675–684. <https://doi.org/10.1007/s10483-010-1302-9>
- [6] Yih, K. A. (1999). Coupled heat and mass transfer by free convection over a truncated cone in porous media: VWT/VWC or VHF/VMF. *Acta mechanica*, 137(1), 83–97. <https://doi.org/10.1007/BF01313146>
- [7] Murthy, P. V. S. N., & Singh, P. (2000). Thermal dispersion effects on non-Darcy convection over a cone. *Computers & mathematics with applications*, 40(12), 1433–1444. [https://doi.org/10.1016/S0898-1221\(00\)00251-0](https://doi.org/10.1016/S0898-1221(00)00251-0)
- [8] Roy, S., & Anilkumar, D. (2004). Unsteady mixed convection from a rotating cone in a rotating fluid due to the combined effects of thermal and mass diffusion. *International journal of heat and mass transfer*, 47(8), 1673–1684. <https://doi.org/10.1016/j.ijheatmasstransfer.2003.10.028>
- [9] Takhar, H. S., Chamkha, A. J., & Nath, G. (2004). Effect of thermophysical quantities on the natural convection flow of gases over a vertical cone. *International journal of engineering science*, 42(3), 243–256. <https://doi.org/10.1016/j.ijengsci.2003.07.005>
- [10] Singh, P. J., & Roy, S. (2007). Unsteady mixed convection flow over a vertical cone due to impulsive motion. *International journal of heat and mass transfer*, 50(5), 949–959. <https://doi.org/10.1016/j.ijheatmasstransfer.2006.08.011>
- [11] Kumari, M., & Nath, G. (2009). Natural convection from a vertical cone in a porous medium due to the combined effects of heat and mass diffusion with non-uniform wall temperature/concentration or heat/mass flux and suction/injection. *International journal of heat and mass transfer*, 52(13), 3064–3069. <https://doi.org/10.1016/j.ijheatmasstransfer.2008.10.037>
- [12] Cheng, C.-Y. (2009). Nonsimilar boundary layer analysis of double-diffusive convection from a vertical truncated cone in a porous medium with variable viscosity. *Applied mathematics and computation*, 212(1), 185–193. <https://doi.org/10.1016/j.amc.2009.02.012>

- [13] Chio, S. U. S., & Eastman, J. A. (1995). Enhancing thermal conductivity of fluid with nanoparticles. *Developments and applications of non-newtonian flow, da siginer and hp wang eds., fed*, 231, 99. [https://www.researchgate.net/publication/236353373\\_Enhancing\\_thermal\\_conductivity\\_of\\_fluids\\_with\\_nanoparticles](https://www.researchgate.net/publication/236353373_Enhancing_thermal_conductivity_of_fluids_with_nanoparticles)
- [14] Khanafer, K., Vafai, K., & Lightstone, M. (2003). Buoyancy-driven heat transfer enhancement in a two-dimensional enclosure utilizing nanofluids. *International journal of heat and mass transfer*, 46(19), 3639–3653. [https://doi.org/10.1016/S0017-9310\(03\)00156-X](https://doi.org/10.1016/S0017-9310(03)00156-X)
- [15] Buongiorno, J. (2005). Convective Transport in Nanofluids. *Journal of heat transfer*, 128(3), 240–250. <https://doi.org/10.1115/1.2150834>
- [16] Daungthongsuk, W., & Wongwises, S. (2007). A critical review of convective heat transfer of nanofluids. *Renewable and sustainable energy reviews*, 11(5), 797–817. <https://doi.org/10.1016/j.rser.2005.06.005>
- [17] Oztop, H. F., & Abu-Nada, E. (2008). Numerical study of natural convection in partially heated rectangular enclosures filled with nanofluids. *International journal of heat and fluid flow*, 29(5), 1326–1336. <https://doi.org/10.1016/j.ijheatfluidflow.2008.04.009>
- [18] Nield, D. A., & Kuznetsov, A. V. (2009). The Cheng–Minkowycz problem for natural convective boundary-layer flow in a porous medium saturated by a nanofluid. *International journal of heat and mass transfer*, 52(25), 5792–5795. <https://doi.org/10.1016/j.ijheatmasstransfer.2009.07.024>
- [19] Nield, D. A., & Kuznetsov, A. V. (2011). The Cheng–Minkowycz problem for the double-diffusive natural convective boundary layer flow in a porous medium saturated by a nanofluid. *International journal of heat and mass transfer*, 54(1), 374–378. <https://doi.org/10.1016/j.ijheatmasstransfer.2010.09.034>
- [20] Ahmad, S., & Pop, I. (2010). Mixed convection boundary layer flow from a vertical flat plate embedded in a porous medium filled with nanofluids. *International communications in heat and mass transfer*, 37(8), 987–991. <https://doi.org/10.1016/j.icheatmasstransfer.2010.06.004>
- [21] Khan, W. A., & Pop, I. (2010). Boundary-layer flow of a nanofluid past a stretching sheet. *International journal of heat and mass transfer*, 53(11), 2477–2483. <https://doi.org/10.1016/j.ijheatmasstransfer.2010.01.032>
- [22] Kuznetsov, A. V., & Nield, D. A. (2010). Natural convective boundary-layer flow of a nanofluid past a vertical plate. *International journal of thermal sciences*, 49(2), 243–247. <https://doi.org/10.1016/j.ijthermalsci.2009.07.015>
- [23] Kuznetsov, A. V., & Nield, D. A. (2010). Effect of local thermal non-equilibrium on the onset of convection in a porous medium layer saturated by a nanofluid. *Transport in porous media*, 83(2), 425–436. <https://doi.org/10.1007/s11242-009-9452-8>
- [24] Alqurashi, F., & Hassan, S. (2024). Artificial intelligence neural network modeling of radiative nanofluid flow via a vertical cone in porous substance with activation energy effect. *Ain shams engineering journal*, 15(6), 102718. <https://doi.org/10.1016/j.asej.2024.102718>
- [25] Gomathi, N., & Poulomi, D. (2024). Entropy optimization on EMHD Casson Williamson penta-hybrid nanofluid over porous exponentially vertical cone. *Alexandria engineering journal*, 108, 590–610. <https://doi.org/10.1016/j.aej.2024.07.092>
- [26] Kodi, R., Ganteda, C., Dasore, A., Kumar, M. L., Laxmaiah, G., Hasan, M. A., ... & Abdul Razak. (2023). Influence of MHD mixed convection flow for maxwell nanofluid through a vertical cone with porous material in the existence of variable heat conductivity and diffusion. *Case studies in thermal engineering*, 44, 102875. <https://doi.org/10.1016/j.csite.2023.102875>
- [27] Ragulkumar, E., Sambath, P., & Chamkha, A. J. (2023). Natural convective dissipative different nanofluid flow past a vertical cone with heat and mass transfer. *Waves in random and complex media*, 0(0), 1–27. <https://doi.org/10.1080/17455030.2023.2226225>
- [28] Yashodha, S., Ganga, B., Abdul Hakeem, A. K., & Sivasankaran, S. (2023). Convective Flow of Water-Ethylene Glycol (50: 50) Based Nanofluid Over a Spinning Down-Pointing Vertical Cone in a Darcy Porous Medium. *Journal of nanofluids*, 12(8), 2228–2236. <https://doi.org/10.1166/jon.2023.2086>
- [29] Rana, P., Kumar, A., & Pippal, S. (2023). The Cheng–Minkowycz problem for quadratic convective and radiative heat transfer in a nanofluid saturated porous medium: A revised model. *Case studies in thermal engineering*, 43, 102802. <https://doi.org/10.1016/j.csite.2023.102802>

- [30] Alsabery, A. I., Abosinnee, A. S., Ismael, M. A., Chamkha, A. J., & Hashim, I. (2024). Natural convection inside nanofluid superposed wavy porous layers using LTNE model. *Waves in random and complex media*, 34(5), 4352–4380. <https://doi.org/10.1080/17455030.2021.1989519>
- [31] Zhao, X., Nasir, M., Al-Dossari, M., Ashiq, M., Salman Kausar, M., Waqas, M., & Abdullaev, S. (2024). Chemically reactive magnetized flow of viscoplastic nanofluid through a vertical cone considering non-Darcy porous media. *Engineering science and technology, an international journal*, 59, 101853. <https://doi.org/10.1016/j.jestch.2024.101853>
- [32] Xu, H., Awwad, F. A., Ismail, E. A. A., & Khan, W. (2025). Mathematical model and stability of SWCNT- and MWCNT-based nanofluid flow with thermal and chemically reactive effects inside a porous vertical cone. *Frontiers in chemistry*, 12, 1–13. <https://doi.org/10.3389/fchem.2024.1463778>
- [33] Nabwey, H. A., Armaghani, T., Azizimehr, B., Rashad, A. M., & Chamkha, A. J. (2023). A Comprehensive review of nanofluid heat transfer in porous media. *Nanomaterials*, 13(5), 937. <https://doi.org/10.3390/nano13050937>
- [34] Liao, S. J. (2003). *Beyond perturbation: Introduction to homotopy analysis method*. Chapman and Hall/CRC Press. <https://doi.org/10.1016/B978-0-08-042843-7.X5000-4%0A%0A>